



Modeling and Optimization of Anethole Ultrasound-Assisted Extraction from Fennel Seeds using Artificial Neural Network

Hojatollah Moradi^a, Hossein Bahmanyar^{a,*}, Hedayat Azizpour^{a,b,†}, Nariman Rezamandi^a, Seyed Mohsen Mirdehghan Ashkezari^a

- a. Surface Phenomenon and Liquid-Liquid Extraction Research Lab, School of Chemical Engineering, College of Engineering, Postal Code: 1417466191, University of Tehran, Iran
b. Department of Chemical Engineering, Fouman Faculty of Engineering, College of Engineering, Postal Code: 1417466191, University of Tehran, Iran

Received: 24 April 2020, Revised: 11 May 2020, Accepted: 16 May 2020
© University of Tehran 2020

Abstract

Extraction of essential oils from medicinal plants has received researcher's attention as it has a wide variety of applications in different industries. In this study, ultrasonic method has been used to facilitate the extraction of active ingredient anethole from fennel seeds. Effect of different parameters like extraction time (20, 40, and 60 min), power (80, 240, and 400 Watts) and solid particle size (0.3, 1, and 1.7 mm) on the anethole extraction yield have been studied. The box-Behnken design method has been used for the design of experiments to reduce the number of experiments. A second-degree polynomial was proposed to predict the relationship between independent variables and the dependent variable. An artificial neural network was trained with experimental data to provide another model for the system. Optimal results achieved when using the Levenberg-Marquardt back-propagation algorithm, Logsig, and Tansig transfer functions for hidden and output layers and the number of 10 neurons in the hidden layer. Coefficient of determination, sum of squared errors, root of mean square error, and absolute average deviation were found to be 0.9933, 0.0199, 0.0059, and 2.1944 for the ANN model and 0.9851, 0.0425, 0.0059 and 2.1944 for the design of experiment (DOE) model, respectively.

Keywords:

Artificial Neural Network, Box-Behnken Design, Essential Oils, Surface Methodology, Ultrasound

Introduction

Umbelliferae (*Apiaceae*) is the biggest known family of flowering plants, which was studied by botanists in the late 1500s [1]. Using medicinal plants to prevent and cure diseases was quite prevalent until the 16th century and was considered the most reliable way to cure different illnesses. In recent years, due to the high price and various side effects of chemical drugs, using medicinal plants has soared again. Fennel (*Foeniculum vulgare*) is a green herbaceous plant from the family of Umbelliferae, which is cultivated in a lot of countries for its many different uses [2]. Fennel contains 10% oil, carbohydrates, mucilage, and roughly 4% essential oil [3]. Fennel's essential oil is commonly used in the pharmaceutical, food, and hygiene industry. Anethole is one of the most important (active substances/ingredients) in fennel [4]. The anethole

* Corresponding author:

Email: hbahmany@ut.ac.ir (H. Bahmanyar)

† Corresponding author:

Email: h.azizpour@ut.ac.ir (H. Azizpour)

in the fennel's essential oil has strong anticancer capabilities and can reduce spasm in the digestive system and improve the quality of digestion by stimulating digestive juice secretion [5,6].

Conventional methods of extraction require long residence time and great quantities of solvents; as a result, researchers are trying to find new techniques to reduce extraction time, the solvent used, and pollution. In experimental studies, using the "one-factor-at-a-time" approach is time-consuming and burdensome and does not always succeed at determining optimum conditions [7]. There are various methods for extracting essential oils from plant seeds, some of which are: superheated steam distillation [3,8], solvent extraction [9], extraction using microwaves [10], supercritical fluid extraction [11] and ultrasound-assisted extraction [12]. Ultrasound-assisted extraction is one of the novel effective methods of extracting essential oil from plants. The main advantages of using this method are its low cost and simplicity of the required equipment. Because of the limitations of theoretical models, Empirical models are usually used to describe the interactions of model variables on each other.

Response surface methodology (RSM) and artificial neural network (ANN) are efficient methods for empirical modeling [7]. Response surface methodology was first introduced by George E. P. Box and K. B. Wilson in 1951 [13]. Response surface methodology is a statistical technique that utilizes specific methods to determine an approximate relationship between input and output variables. [14]. This method is also capable of determining the effect of different independent variables on the dependent variable [15]. Mokhtari et al. [16] investigated the extraction of anethole from fennel seeds by supercritical CO₂ with the addition of ethanol as a co-solvent and modeled the system by implementation of genetic algorithm and response surface methodology.

ANN can be defined as a group of computational nodes named neurons that are linked together with weighted connections [17]. One of the most significant characteristics of ANN is its training capability, which makes it suitable for modeling complex, nonlinear systems [18,19]. Currently, ANN is known as an effective tool for predicting food properties and process optimization [20,21]. Khajenoori and Haghghi Asl [22] studied the subcritical solvent extraction of trans-anethole, using ANN. They used temperature, flow rate, and mean particle size as input variables and extraction yield as the output. Optimum results reported when using one hidden layer with five neurons.

Since conducting experiments is time-consuming and difficult, a modeling method is usually used to reduce extraction time and expenses, optimize the process, and predict the behavior of variables in different situations. In this work, ultrasound-assisted extraction of anethole was modeled using ANN and the results were compared with the design of experiment (DOE) model. In the modeling, three parameters of time, power, and particle size were used as independent variables along with the extraction yield as the dependent variable.

Methodology

Fennel seeds were ground using a mill and were divided into three sizes of 0.3, 1, and 1.7 mm, then 5 grams of each were mixed with 70% w/w ethanol-water solution with a ratio of 1 to 15 (75 mL solution). To prevent degradation, a cold-water bath inside the ultrasonic chamber was used to keep the temperature constant. The ultrasonic device used was horn-type cell disruptor UP400S from Hielscher, Germany, with a nominal power of 400 Watts and a frequency of 24 kHz. Ultrasonic waves produced in the solution increases the mass transfer from the particles significantly by inducing a phenomenon known as cavitation. The intensity of these ultrasound waves can be changed by adjusting the power input of the device from 20 to 100 %. After extraction with ultrasound, solid particles were separated with a filter, and the solution was placed in a centrifuge for 15 minutes. The essential oil obtained from the solution was then

dried to minimize errors in mass chromatography analysis. The extraction yield was calculated according to the following formula:

$$\text{Extraction yield} = \frac{\text{Weight of essential oil extracted (g)}}{\text{Weight of dried sample (g)}}$$

Separation and identification of compounds in the essential oil of fennel seeds were done using Agilent 7890A GC/MS.

Modeling

Accuracy of RSM and ANN models was assessed using root mean square error, sum of square errors, coefficient of determination, and absolute average derivation .

$$\text{RMSE} = \sqrt{\frac{\sum_{i=1}^n (y_{i,\text{pred}} - y_{i,\text{exp}})^2}{n}} \quad (1)$$

$$\text{SSE} = \sum_{i=1}^n (y_{i,\text{pred}} - y_{i,\text{exp}})^2 \quad (2)$$

$$R^2 = 1 - \frac{\sum_{i=1}^n (y_{i,\text{pred}} - y_{i,\text{exp}})^2}{\sum_{i=1}^n (y_{i,\text{exp}} - y_m)^2} \quad (3)$$

$$\text{AAD} = \left[\frac{\sum_{i=1}^n (|y_{i,\text{exp}} - y_{i,\text{pred}}| / y_{i,\text{exp}})}{n} \right] \times 100 \quad (4)$$

where n is the number of experimental data, $y_{i,\text{pred}}$ is the predicted yield, $y_{i,\text{exp}}$ is the experimental yield and y_m is the mean experimental yield.

BBD method was used to evaluate the effect of time, power, and particle size variables on the response surface and optimization of anethole extraction from fennel seeds. Using the BBD method, the experiment was designed in 17 tests and 3 levels. Table 1 shows independent variables and their range. A second-degree polynomial describes the relation between the dependent variable (yield) and independent variables (time, power, and particle size).

$$Y = b_0 + \sum_{i=1}^3 b_i X_i + \sum_{i=1}^3 b_{ii} X_i^2 + \sum_{i=1}^2 \sum_{j=i+1}^3 b_{ij} X_i X_j \quad (5)$$

where Y identifies the response; b_0 , b_i , b_j , and b_{ij} are coefficients of a second-degree polynomial, and X_i and X_j are independent variables. Design and analysis of the DOE model were done using Design-Expert 7.0.0 (Stat-Ease Inc., Minneapolis).

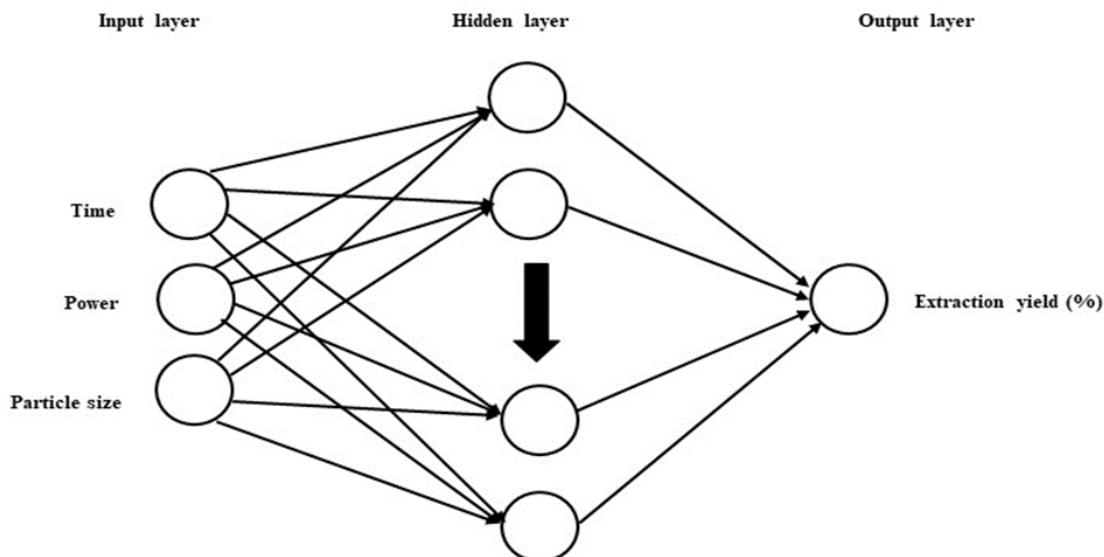
ANN consists of input, output, and hidden layers, which are interconnected by weighted and biased connections. In the modeling of this system, the neural network has three inputs (extraction time, power, and particle size) and one output (extraction yield). The structure of the network is shown in Fig. 1, which contains n neurons in the hidden layer. Extraction yield values are normalized using [17].

$$Y_{\text{norm}} = 0.8 \times \frac{Y - Y_{\text{min}}}{Y_{\text{max}} - Y_{\text{min}}} + 0.1 \quad (6)$$

where Y_{norm} is the normalized value of Y (extraction yield of anethole); and Y_{min} and Y_{max} are minimum and maximum values of Y , respectively. From all the experimental data, 70 percent are used for training, 15 percent for testing, and 15 percent for validation. Experimental data used for training of the neural network model, Actual and predicted values of extraction yield are given in Table 2. Modeling using ANN is implemented in MATLAB (R2019b).

Table 1. Independent variables

Independent variables		Levels		
1	Time (min)	20	40	60
2	Power (Watt)	80	240	400
3	Particle size (mm)	0.3	1	1.7

**Fig. 1.** Schematic representation of ANN

Results and Discussions

Response Surface Methodology

Designed tests and predicted responses using BBD and ANN methods are presented in [Table 2](#). Using the obtained results, an empirical relation is derived that shows the effect of independent variables on the extraction yield ([Eq. 7](#)). To find the best equation, fit statistics of various models were calculated and compared. According to [Table 3](#), the quadratic model has superior performance compared to linear and two-factor interaction (2FI) models. To further improve the validity of the quadratic model, parameters with high probabilities of error (P-values) were removed from the model. Calculated P-values and coefficients of the second-degree polynomial are given in [Table 4](#). P-value is a parameter that specifies the statistical significance of a variable in the model. A P-value greater than 0.05 means that there is no association between the changes in the variable and response. As shown in [Table 4](#), P-values for b_1^2 and interaction terms (b_1b_2 , b_1b_3 , b_2b_3) are higher than 0.05, which indicates that they are not significant and can be removed from the equation to improve the validity of the model. As can be seen in [Table 3](#), the Modified Quadratic model ([Eq. 7](#)) has a greater predicted coefficient of determination and lower predicted residual error sum of squares (PRESS) value, which suggests it has a higher predictive capability and less chance of overfitting.

$$\text{yield} = 1.57236 + 0.01475 \times \text{Time} - 0.0005 \times \text{Power} - 1.4069 \times \text{Particle size} - 0.000003 \times \text{Power}^2 + 0.37755 \times \text{Particle size}^2 \quad (7)$$

[Table 4](#) shows the result of the analysis of variance (ANOVA) on the yield of anethole extraction. According to the analysis of variance, the F-value of the model (regression) after removing the parameter corresponding to Time^2 (F-value = 109.95) was much greater than the tabular F-values with the same degrees of freedom, indicating the significance of the adjustment made.

Table 2. Design of experiment, actual responses and predicted responses of BBD and ANN models

Run No.	Time	Power	Particle size	Response	Predicted BBD	Predicted ANN
1	40	240	1	0.9	0.94	0.947
2	40	240	1	0.96	0.94	0.947
3	20	80	1	0.65	0.74	0.659
4	60	240	0.3	1.51	1.6	1.513
5	40	400	0.3	1.83	1.83	1.828
6	40	240	1	0.94	0.94	0.947
7	20	240	0.3	1.52	1.47	1.513
8	40	240	1	0.98	0.94	0.947
9	20	240	1.7	0.58	0.55	0.581
10	20	400	1	1.09	1.07	1.172
11	60	400	1	1.21	1.2	1.234
12	60	80	1	0.94	0.88	0.994
13	40	80	1.7	0.59	0.6	0.592
14	40	80	0.3	1.55	1.51	1.563
15	60	240	1.7	0.7	0.69	0.669
16	40	400	1.7	0.89363333	0.92	0.899
17	40	240	1	0.97	0.94	0.947

Table 3. Fit summary for different models

	Std. Dev.	Adjusted R ²	Predicted R ²	PRESS
Linear	0.1297	0.8733	0.8081	0.4075
2FI	0.1439	0.8440	0.5971	0.8555
Quadratic	0.0534	0.9786	0.8771	0.2610
Modified (Eq. 7)	0.0644	0.9687	0.9385	0.1307

Fig. 2a shows the variation of extraction yield with respect to particle size and power in the time of 40 minutes (Contour plot). As shown in Fig. 2a, in constant power, increasing mesh size (decreasing particle size) will increase anethole extraction yield and in constant particle size, increasing power will increase the yield. As can be seen in this figure, the maximum extraction yield (1.83%) occurs at maximum power (400 W) and minimum particle size (0.3 mm).

Fig. 2b shows the change of extraction yield versus power and time when using mesh size 12 (particle size of 0.3 mm). As shown in this figure, using large particles with low power will cause low extraction yield, even lower than of steam distillation. Referring to prior studies, 8 hours is required to achieve a yield of 1.2 percent in steam distillation [23]. This implies that lower extraction time is one of the benefits of using ultrasound in comparison with conventional methods. It should be noted that temperature should be kept constant during the test at 25 °C since temperature changes during the process can cause the degradation of active ingredients.

Table 4. P-values and parameter estimates from ANOVA analysis

Coefficient	Parameter estimate	P-value
b ₀	1.57236	< 0.0001
b ₁	0.01475	0.0085
b ₂	-0.0005	< 0.0001
b ₃	-1.4069	< 0.0001
b ₁ ²	0.000148	0.0626
b ₂ ²	0.000003	0.0154
b ₃ ²	0.37755	< 0.0001
b ₁ b ₂	-0.000013	0.1551
b ₁ b ₃	0.002321	0.2626
b ₂ b ₃	0.000053	0.8310

Table 5. Analysis of variance (ANOVA) for anethole extraction yield

Source of variations	Regression	Residuals	Total	Lack of fit
Sum of squares	2.0850	0.032	2.12	0.0280
Degree of freedom	6	10	16	6
F-value	109.95	-	-	4.62
P-value	<0.0001	-	-	0.0801

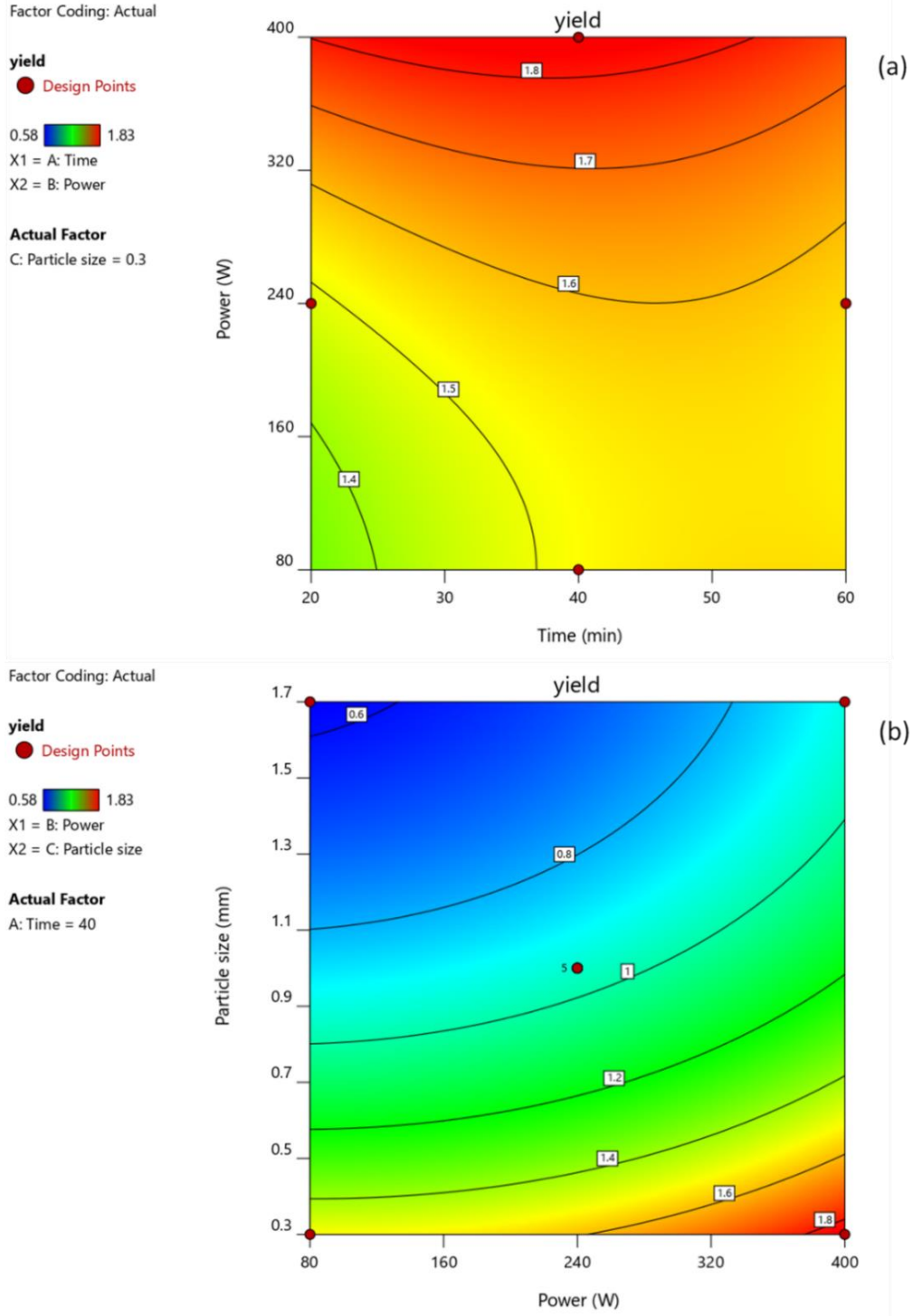


Fig. 2. Contour plots. (a) effect of particle size and power (time = 40 min), (b) effect of power and time (particle size = 0.3 mm)

Artificial Neural Network

Results of the neural network modeling are highly dependent on training algorithms, transfer functions of hidden and output layers, and the number of neurons in the hidden layer [24]. To find the most efficient training algorithm, 8 different training algorithms were tested and compared, when using 8 neurons in the hidden layer and Tansig transfer function for hidden and output layers. According to the values of the coefficient of determination (R^2), R^2_{adj} , root mean square error (RMSE), and sum of squared errors (SSE) presented in Table 6 for 8 different functions, it can be observed that the back-propagation algorithm of Levenberg-Marquardt (LM) has the best performance. Values of R^2 , R^2_{adj} , RMSE, and SSE for LM algorithm are 0.9323, 0.9278, 0.0584 and 0.0514, respectively. In the next step, to find the best transfer function for output and hidden layers, 9 different functions were tested with the LM algorithm and the constant number of 8 neurons in the hidden layer. The best performance was achieved when using Tansig function for output, and Logsig function for the hidden layer. Corresponding values of R^2 , R^2_{adj} , RMSE, and SSE for this model are 0.9657, 0.9634, 0.0486, and 0.0354, respectively, that are shown in Fig. 3. Finally, to find the optimum number of neurons, the number of neurons was changed from 5 to 16 and each model was trained three times. LM training algorithm was used along with Logsig and Tansig transfer functions for the hidden and output layer. Fig. 4 shows R^2 (Fig. 4a), RMSE (Fig. 4b), and SEE (Fig. 4c) for this setting. It is clear from Fig. 4a that the coefficient of determination is the highest when using 10 neurons in the hidden layer ($R^2 = 0.9933$), which indicates the high accuracy of the model in predicting the experimental data. In addition, referring to Fig. 4b and c, the values of RMSE and SEE are 0.0199 and 0.0059, respectively. Table 7 shows the final weights and bias after training the network with optimum settings.

Table 6. Coefficient of determination (R^2), sum of squared errors (SSE), and root mean square error (RMSE) for different training algorithms

Number	Function	Transfer functions hidden layers	Transfer functions output layers	R^2	R^2_{adj}	RMSE	SSE
1	BFG	Tansig	Tansig	0.7777	0.7629	0.1085	0.1766
2	BR	Tansig	Tansig	0.9176	0.9121	0.0581	0.0507
3	CGB	Tansig	Tansig	0.8999	0.8932	0.0766	0.0881
4	CGF	Tansig	Tansig	0.8834	0.8756	0.0884	0.1173
5	CGP	Tansig	Tansig	0.8760	0.8677	0.0828	0.1030
6	LM	Tansig	Tansig	0.9323	0.9278	0.0585	0.0514
7	R	Tansig	Tansig	0.7746	0.7595	0.1145	0.1968
8	RP	Tansig	Tansig	0.8081	0.7953	0.1141	0.1952

Table 7. Weights and the bias of optimum neural network

Neuron	Time	W_1			W_2	$B_2 = -1.7022$
		Power	Particle size	Efficiency Extraction	B_1	
1	0.35252	2.5335	-5.0933	1.054	-6.4739	
2	-2.5718	-5.8248	0.38262	-1.2164	4.3475	
3	-4.1878	0.93488	-3.9704	-0.018265	3.4004	
4	-2.0889	-3.3551	-4.6763	0.41297	1.6292	
5	3.8473	2.5974	-3.4278	1.6732	1.7604	
6	-5.687	0.52662	-1.9351	0.2595	0.37376	
7	-3.1177	-2.7168	-4.3576	0.88449	-1.5488	
8	-5.4538	2.4362	-0.83091	-1.5504	-3.8391	
9	-3.8124	3.54	-2.6635	0.64937	-4.7741	
10	-3.7249	5.5752	-1.6191	1.4514	-5.0982	

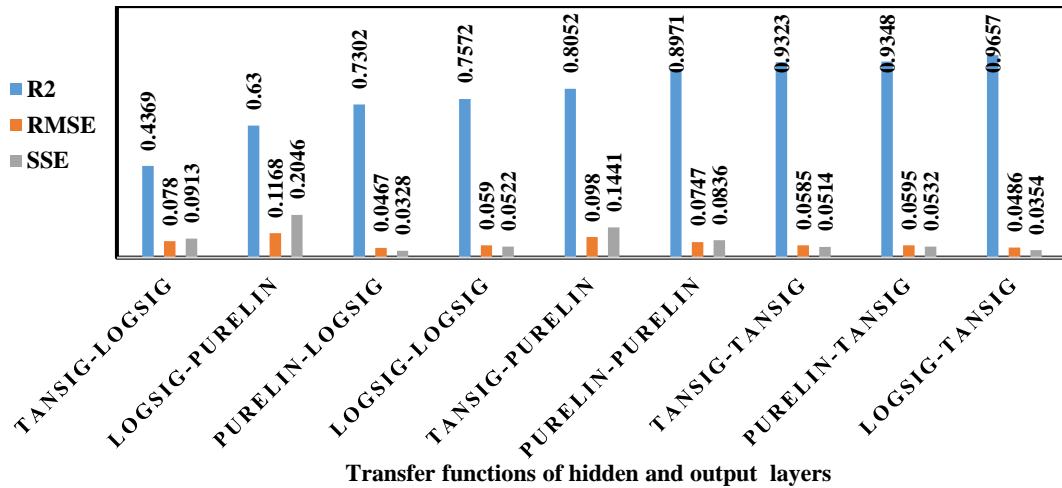


Fig. 3. Coefficient of determination (R²), sum of squared errors (SSE), and root mean square error (RMSE) for finding the optimum transfer function

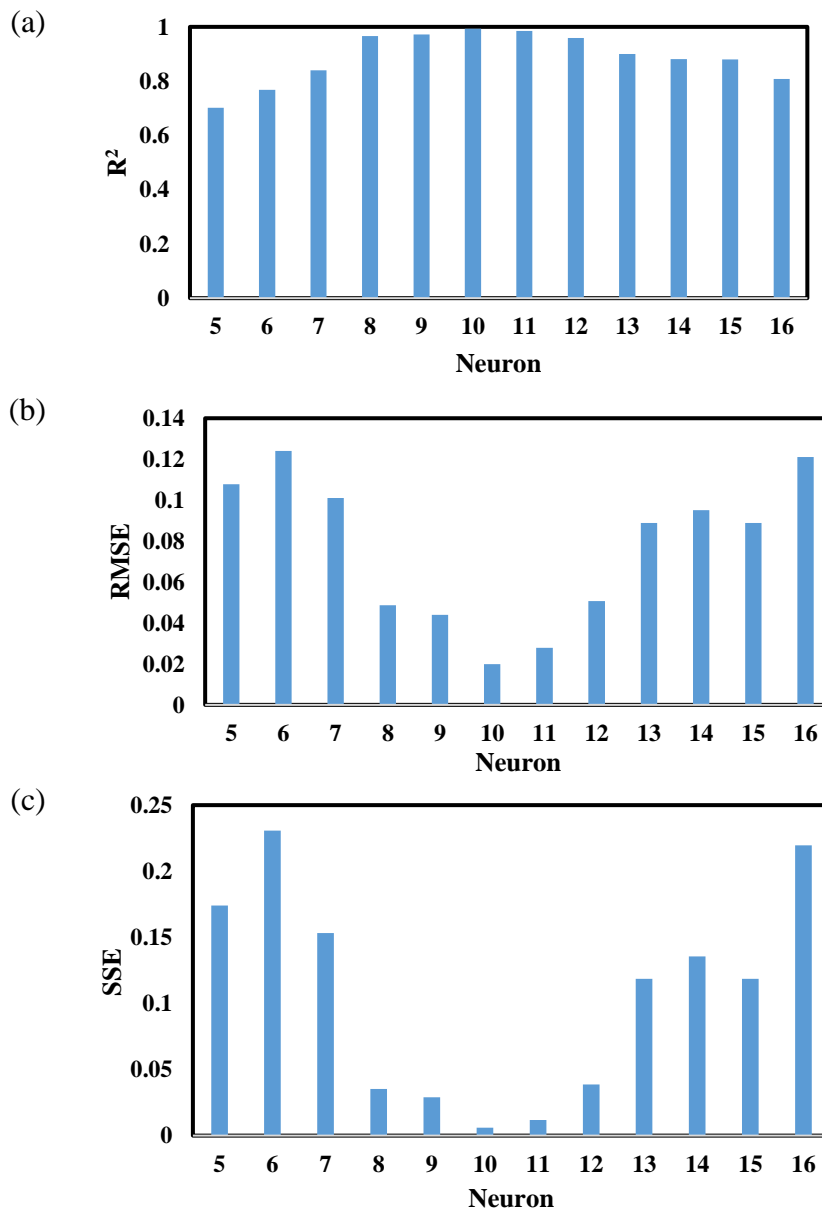


Fig. 4. (a) Coefficient of determination (R²), (b) root mean square error (RMSE) for determining optimum number of neurons in the hidden layer, (c) sum of squared errors (SEE).

After training the neural network with the optimum configuration, predicted extraction yield using ANN and DOE models were compared (Fig. 5). R^2 is 0.9933 and 0.9851 for ANN and DOE models, respectively. Values of RMSE, SSE, and AAD (%) in Table 8 show the higher accuracy of the neural network model over the design of the experiment model.

Table 8. Coefficient of determination, root mean square error, sum of squared errors, and average absolute deviation for ANN and RSM models

Parameters	RSM	ANN
R^2	0.9851	0.9933
RMSE	0.0425	0.0199
SSE	0.0307	0.0059
AAD(%)	3.5099	2.1944

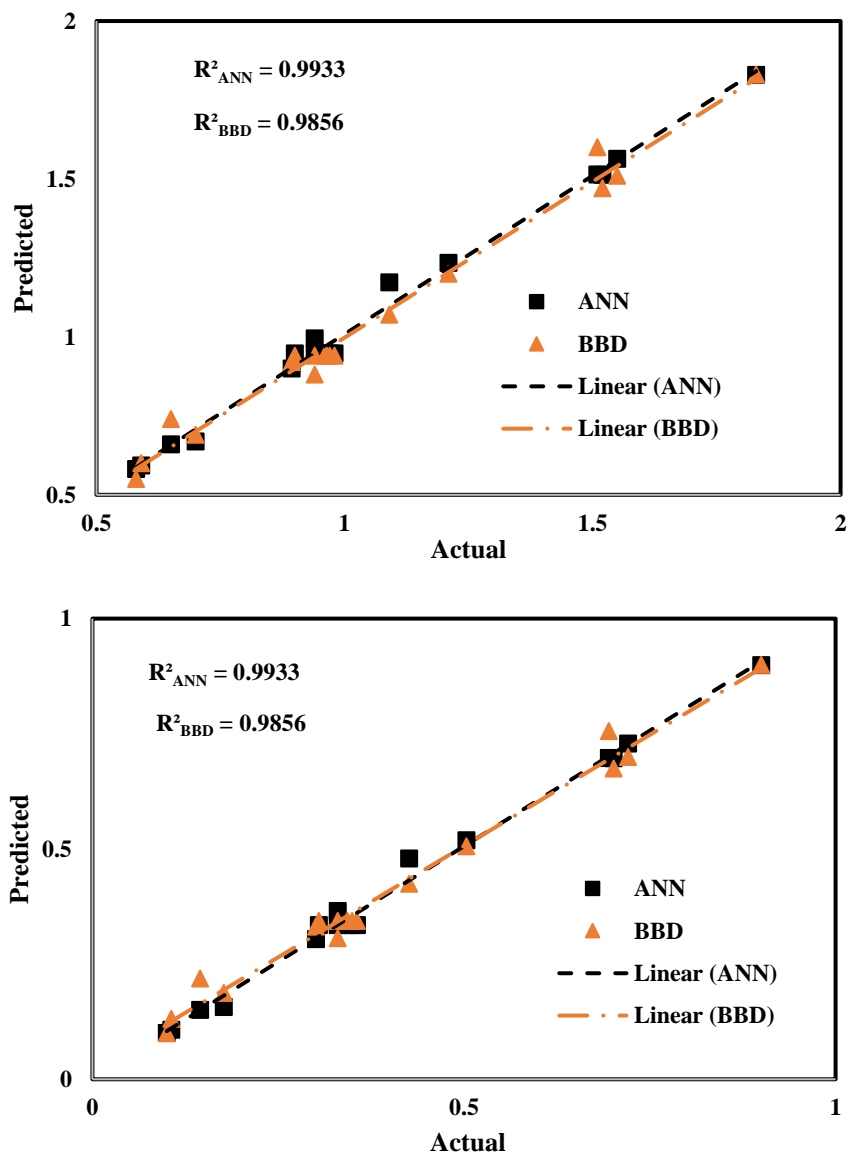


Fig. 5. Predicted extraction yield with neural network model to the predicted yield of design of experiment model.

Conclusions

In this study, the effect of three parameters of extraction time, power, and mean particle size on the ultrasound-assisted extraction yield of anethole from fennel seeds was investigated using ANN and design of experiment method. 17 tests were designed using the BBD experiment design method. Results showed that increasing irradiator power and reducing solid particle size will increase anethole extraction yield and the maximum yield of 1.83 was obtained with the power of 400 Watts and the particle size of 0.3 mm, in the time of 40 minutes. According to the experiments, the best results were obtained when using 10 neurons in the hidden layer. Comparing the average absolute deviation for ANN and DOE methods (2.1994 and 3.5099 for ANN and DOE models, respectively), revealed the superior performance of ANN model in predicting the anethole extraction yield from fennel seeds over the design of experiment method. Excellent agreement between the ANN predicted results and the actual responses ($R^2 = 0.9933$), shows that the ANN was efficient in modeling the non-linear behavior of the system.

Nomenclature

List of abbreviations

ANN	Artificial neural network
DOE	Design of experiment
BBD	Box-Behnken design method
LM	Levenberg-Marquardt
RSM	Response surface methodology
RMSE	Root mean square error
SSE	Sum of squared errors
AAD	Average absolute deviation
R^2	Coefficient of determination

References

- [1] Kunieda S, inventor; Takasago International Corp, assignee. Flavor enhancer, food or beverage containing the flavor enhancer, and method of flavor enhancement. United States patent application US 10/564,437. 2006 Jul 20.
- [2] Mohamad RH, El-Bastawesy AM, Abdel-Monem MG, Noor AM, Al-Mehdar HA, Sharawy SM, El-Merzabani MM. Antioxidant and anticarcinogenic effects of methanolic extract and volatile oil of fennel seeds (*Foeniculum vulgare*). *Journal of Medicinal Food*. 2011 Sep 1;14(9):986-1001.
- [3] Piccaglia R, Marotti M. Characterization of some Italian types of wild fennel (*Foeniculum vulgare* Mill.). *Journal of Agricultural and Food Chemistry*. 2001 Jan 15;49(1):239-44.
- [4] Bilia AR, Flamini GU, Taglioli V, Morelli IV, Vincieri FF. GC-MS analysis of essential oil of some commercial Fennel teas. *Food Chemistry*. 2002 Mar 1;76(3):307-10.
- [5] Oktay M, Gülçin İ, Küfrevioğlu Öİ. Determination of in vitro antioxidant activity of fennel (*Foeniculum vulgare*) seed extracts. *LWT-Food Science and Technology*. 2003 Mar 1;36(2):263-71.
- [6] Shahat AA, Ibrahim AY, Hendawy SF, Omer EA, Hammouda FM, Abdel-Rahman FH, Saleh MA. Chemical composition, antimicrobial and antioxidant activities of essential oils from organically cultivated fennel cultivars. *Molecules*. 2011 Feb;16(2):1366-77.
- [7] Pakravan P, Akhbari A, Moradi H, Azandaryani AH, Mansouri AM, Safari M. Process modeling and evaluation of petroleum refinery wastewater treatment through response surface methodology and artificial neural network in a photocatalytic reactor using poly ethyleneimine (PEI)/titania (TiO₂) multilayer film on quartz tube. *Applied Petrochemical Research*. 2015 Mar 1;5(1):47-59.

- [8] Özel MZ, Göğüş F, Lewis AC. Comparison of direct thermal desorption with water distillation and superheated water extraction for the analysis of volatile components of *Rosa damascena* Mill. using GCxGC-TOF/MS. *Analytica Chimica Acta*. 2006 May 4;566(2):172-7.
- [9] Rodríguez-Solana R, Salgado JM, Domínguez JM, Cortés-Diéguez S. Characterization of fennel extracts and quantification of estragole: Optimization and comparison of accelerated solvent extraction and Soxhlet techniques. *Industrial Crops and Products*. 2014 Jan 1;52:528-36.
- [10] Gedye R, Smith F, Westaway K, Ali H, Baldiseria L. The use of microwave ovens for rapid organic synthesis. *Tetrahedron Letters*. 1986;27(3):279-82.
- [11] Reverchon E. Supercritical fluid extraction and fractionation of essential oils and related products. *The Journal of Supercritical Fluids*. 1997 Apr 14;10(1):1-37.
- [12] Khan MK, Abert-Vian M, Fabiano-Tixier AS, Dangles O, Chemat F. Ultrasound-assisted extraction of polyphenols (flavanone glycosides) from orange (*Citrus sinensis* L.) peel. *Food Chemistry*. 2010 Mar 15;119(2):851-8.
- [13] Del Castillo E. *Process optimization: a statistical approach*. Springer Science & Business Media; 2007 Sep 14.
- [14] Pournejati R, Karbalaei-Heidari HR, Budisa N. Secretion of recombinant archeal lipase mediated by SVP2 signal peptide in *Escherichia coli* and its optimization by response surface methodology. *Protein Expression and Purification*. 2014 Sep 1;101:84-90.
- [15] Zhang C, Daidi FA, Xiaoxuan MA, Yan'e LU, Wenjiao XU, Pengfei GA. Optimization of fermentation process for human-like collagen production of recombinant *Escherichia coli* using response surface methodology. *Chinese Journal of Chemical Engineering*. 2010 Feb 1;18(1):137-42.
- [16] Mokhtari L, Ghoreishi SM. Supercritical carbon dioxide extraction of trans-anethole from *Foeniculum vulgare* (fennel) seeds: Optimization of operating conditions through response surface methodology and genetic algorithm. *Journal of CO₂ Utilization*. 2019 Mar 1;30:1-0.
- [17] Salajegheh E, Gholizadeh S. Optimum design of structures by an improved genetic algorithm using neural networks. *Advances in Engineering Software*. 2005 Nov 1;36(11-12):757-67.
- [18] Ameer K, Chun BS, Kwon JH. Optimization of supercritical fluid extraction of steviol glycosides and total phenolic content from *Stevia rebaudiana* (Bertoni) leaves using response surface methodology and artificial neural network modeling. *Industrial Crops and Products*. 2017 Dec 15;109:672-85.
- [19] Nazghelichi T, Aghbashlo M, Kianmehr MH. Optimization of an artificial neural network topology using coupled response surface methodology and genetic algorithm for fluidized bed drying. *Computers and Electronics in Agriculture*. 2011 Jan 1;75(1):84-91.
- [20] Sefat MY, Borgaee AM, Beheshti B, Bakhoda H. Modelling energy efficiency in broiler chicken production units using artificial neural network (ANN). *International Journal of Natural and Engineering Sciences*. 2014;8(1):7-14.
- [21] Gharagheizi F, Eslamimanesh A, Mohammadi AH, Richon D. Determination of critical properties and acentric factors of pure compounds using the artificial neural network group contribution algorithm. *Journal of Chemical & Engineering Data*. 2011 May 12;56(5):2460-76.
- [22] Khajenoori M, ASL AH. Prediction of Trans-anethole Extraction Yield from *Pimpinella Anisum* Seeds Using Artificial Neural Network. *Uluslararası Doğa ve Mühendislik Bilimleri Dergisi*.;12(1):37-41.
- [23] Damayanti A, Setyawan E. Essential oil extraction of fennel seed (*Foeniculum vulgare*) using steam distillation. *International Journal of Science and Engineering*. 2012;3(2):12-4.
- [24] Teslić N, Bojanić N, Rakić D, Takači A, Zeković Z, Fišteš A, Bodroža-Solarov M, Pavlić B. Defatted wheat germ as source of polyphenols—Optimization of microwave-assisted extraction by RSM and ANN approach. *Chemical Engineering and Processing-Process Intensification*. 2019 Sep 1;143:107634.



This article is an open-access article distributed under the terms and conditions of the Creative Commons Attribution (CC-BY) license.